Effect of running coupling on photon emission from quark gluon plasma

Mahatsab Mandal and Pradip Roy
Saha Institute of Nuclear Physics, 1/AF Bidhannagar, Kolkata 700064, India

Sukanya Mitra and Sourav Sarkar
Variable Energy Cyclotron Centre, 1/AF Bidhannagar, Kolkata 700064, India
(Received 10 January 2012; revised manuscript received 9 April 2012; published 21 June 2012)

We discuss the role of running coupling on the thermal photon yield from quark gluon plasma. It is shown that the photon production rate from the partonic phase is considerably enhanced when running coupling is considered with respect to a fixed value. However, we show by explicit evaluation that although this difference survives the space-time evolution the experimental data cannot distinguish between the two once the hard contribution, which is an essential component of the photon production mechanism, is added.

DOI: 10.1103/PhysRevC.85.067901 PACS number(s): 25.75.−q, 12.38.Mh

Detection of quark gluon plasma (QGP) in heavy-ion collisions has received significant attention in recent years. Among possible signals, electromagnetic probes are one of the most promising tools to characterize the initial state of the collisions [1]. Owing to their weak coupling with the constituents of the system they tend to escape almost unscattered. In fact, photons (dileptons as well) can be used to determine the initial temperature, or equivalently the equilibration time. By comparing the initial temperature with the transition temperature from lattice QCD, one can infer whether QGP is produced.

Photons are produced at various stages (i) from initial hard scattering of partons, (ii) from scattering of charged particles in the thermal medium (QGP and hadronic matter), and (iii) from π^0 and η^0 decays. If this decay contribution is subtracted from the total photon yield, what is left is the direct (excess) photons. The thermal photon rate due to Compton and annihilation processes in a quark gluon plasma has been calculated by several authors over the past two decades [2–6]. In all these calculations the strong coupling, α_s, is treated as constant or a function of temperature T. However, in the case of relativistic heavy-ion collisions, apart from temperature there is also the momentum scale k. One has to take into account the case when $k \sim T$ and treat α_s to be a function of both k and T [7]. By incorporating this fact it is shown that the energy loss is a factor of 2–6 more than the case when α_s is constant [7,8]. The energy loss calculation using running coupling and reduced screening mass in Ref. [8] explains single-electron R_{AA} quite well. It is the purpose of this Brief Report to treat the strong coupling as running and apply it to the case of thermal photon production from QGP.

The lowest-order processes for photon emission from QGP are the Compton scattering $[q(\bar{q})\,g \to q(\bar{q})\,\gamma]$ and annihilation $(q\,\bar{q} \to g\,\gamma)$ processes. The total cross section diverges in the limit t or $u \to 0$. These singularities have to be shielded by thermal effects in order to obtain infrared safe calculations. It was argued in Ref. [9] that the intermediate quark acquires a thermal mass in the medium, whereas the hard thermal loop (HTL) approach of Ref. [3] shows that very soft modes are suppressed in a medium providing a natural cutoff $k_c \sim gT$. We assume that the singularities can be shielded by the introduction of thermal masses for the participating partons. The differential cross sections for Compton and annihilation processes are given by [10]

$$\frac{d\sigma(qg \to q\gamma)}{d\hat{t}} = \frac{1}{6}\left(\frac{e_q}{e}\right)^2 \frac{8\pi\alpha_s\alpha_e}{(\hat{s}-m^2)^2}\left(\frac{m^2}{\hat{s}-m^2}+\frac{m^2}{\hat{u}-m^2}\right)^2 + \left(\frac{m^2}{\hat{s}-m^2}+\frac{m^2}{\hat{u}-m^2}\right) - \frac{1}{4}\left(\frac{\hat{s}-m^2}{\hat{u}-m^2}+\frac{\hat{u}-m^2}{\hat{s}-m^2}\right) \tag{1}$$

and

$$\frac{d\sigma(q\bar{q} \to g\gamma)}{d\hat{t}} = -\frac{4}{9}\left(\frac{e_q}{e}\right)^2 \frac{8\pi\alpha_s\alpha_e}{\hat{s}(\hat{s}-4m^2)}\left(\frac{m^2}{\hat{t}-m^2}+\frac{m^2}{\hat{u}-m^2}\right)^2 + \left(\frac{m^2}{\hat{t}-m^2}+\frac{m^2}{\hat{u}-m^2}\right) - \frac{1}{4}\left(\frac{\hat{t}-m^2}{\hat{u}-m^2}+\frac{\hat{u}-m^2}{\hat{t}-m^2}\right), \tag{2}$$

where m is the in-medium thermal quark mass, $m^2 \equiv {m_{\rm th}}^2 = 2\pi\alpha_s T^2/3$, and α_e and α_s are the electromagnetic fine-structure and the strong-coupling constants, respectively. The static photon rate in $1+2 \to 3+\gamma$ can be written as [1]

$$\frac{dN}{d^4x d^2p_T dy} = \frac{\mathcal{N}_i}{(2\pi)^7 E}\int d\hat{s}d\hat{t}|\mathcal{M}_i|^2 \times \int dE_1 dE_2 \times \frac{f_1(E_1)f_2(E_2)[1+f_3(E_3)]}{\sqrt{a{E_2}^2+2bE_2+c}}, \tag{3}$$

where

$$\begin{aligned} a &= -\left(\hat{s}+\hat{t}-{m_2}^2-{m_3}^2\right)^2, \\ b &= E_1\left(\hat{s}+\hat{t}-{m_2}^2-{m_3}^2\right)\left({m_2}^2-\hat{t}\right) \\ &\quad + E\left[\left(\hat{s}+\hat{t}-{m_2}^2-{m_3}^2\right)\left(\hat{s}-{m_1}^2-{m_2}^2\right)\right. \\ &\quad \left. -2{m_1}^2\left({m_2}^2-\hat{t}\right)\right], \\ c &= -{E_1}^2\left({m_2}^2-\hat{t}\right)^2 - 2E_1E\left[2{m_2}^2\left(\hat{s}+\hat{t}-{m_2}^2-{m_3}^2\right)\right. \\ &\quad \left. -\left({m_2}^2-\hat{t}\right)\left(\hat{s}-{m_1}^2-{m_2}^2\right)\right] \end{aligned}$$

$$
\begin{aligned}
&- E^2\left[\left(\hat{s} - {m_1}^2 - {m_2}^2\right)^2 - 4{m_1}^2{m_2}^2\right] \\
&- \left(\hat{s} + \hat{t} - {m_2}^2 - {m_3}^2\right)\left({m_2}^2 - \hat{t}\right) \\
&\times \left(\hat{s} - {m_1}^2 - {m_2}^2\right) + {m_2}^2\left(\hat{s} + \hat{t} - {m_2}^2 - {m_3}^2\right)^2 \\
&+ {m_1}^2\left({m_1}^2 - \hat{t}\right)^2,
\end{aligned}
$$

$$
E_{1,\min} = \frac{\hat{s} + \hat{t} - {m_2}^2 - {m_3}^2}{4E} + \frac{E{m_1}^2}{\hat{s} + \hat{t} - {m_2}^2 - {m_3}^2},
$$

$$
E_{2,\min} = \frac{E{m_2}^2}{{m_2}^2 - \hat{t}} + \frac{{m_2}^2 - \hat{t}}{4E},\ E_{2,\max} = -\frac{b}{a} + \frac{\sqrt{b^2 - ac}}{a}.
$$

The function $\mathcal{M}_i$ represents the amplitude for Compton or annihilation processes. The overall degeneracy factor $\mathcal{N}_i = 320/3$ and 20 for Compton and annihilation processes, respectively, involving u and d quarks.

As mentioned earlier, the infrared cutoff is fixed by plasma effects, where only the medium part is considered, completely neglecting the vacuum contribution leading to ambiguity in the calculation of the cross section at finite-temperature QCD. If the latter part is taken into account the strong coupling should be running. Thus for any consistent calculation one has to take this fact into consideration. We have in that case $\alpha_s = \alpha_s(k, T)$ where $k = \sqrt{|t|}$.

Photons from thermal hadronic matter also make up an essential component of the total photon yield from heavy-ion collisions. These are emitted in reactions between charged hadrons and in the radiative decays of unstable hadrons [1,11,12]. In this work, we used the amplitudes of photon-producing reactions involving the π, ρ, ω, η, K, and K^* mesons obtained in Ref. [13].

The hard photon contribution can be calculated by perturbative QCD (pQCD). To calculate photon production from reactions of the type $h_A\, h_B \to \gamma\, X$ (where h_A, h_B refer to hadrons), we assume that the energy is such that the partonic degrees of freedom become relevant and they behave incoherently. The cross section for this process can then be written in terms of the elementary parton-parton cross section multiplied by the partonic flux which depends on the parton distribution functions [14]. The energy scale for this to happen (i.e., the factorization scale) is denoted by Q^2, the square of the momentum transfer of the reaction. Starting with two-body scattering at the partonic level the differential cross section for the reaction of the above type can be written as [15]

$$
\begin{aligned}
\frac{d\sigma_{\gamma,\text{hard}}}{d^2 p_T dy} &= K \sum_{abc} \int_{x_a^{\min}}^{1} dx_a\, G_{a/h_A}(x_a, Q^2)\, G_{b/h_B}(x_b, Q^2) \\
&\times \frac{2}{\pi} \frac{x_a x_b}{2x_a - x_T e^y} \frac{d\sigma}{d\hat{t}}(ab \to \gamma c),
\end{aligned} \tag{4}
$$

where $x_T = 2p_T/\sqrt{s}$ and the factor K is introduced to take into account the higher-order effects. A few comments about the K factor are in order here. The cross section in the above expression is calculated perturbatively to leading order (LO) in the strong coupling. In cases where the next-to-leading-order (NLO) terms are comparable to the LO terms the K factor defined as NLO/LO is introduced in the LO computations to bring in the essence of the NLO terms. It was shown in Ref. [16] that K depends on the choice of the momentum scale, the parton distribution functions, and the shadowing effect, and its value lies between 2 and 3. In the present calculation we take $K \sim 2.5$.

We also include photons from fragmentation process. This is accomplished by introducing the fragmentation function, $D_{\gamma/c}(z, Q^2)$, which when multiplied by dz gives the probability for obtaining a photon from parton c, z being the fractional momentum carried by the photon. Once the photon production cross section is obtained from a hadron-hadron collision, we can determine the direct photon production rates due to hard scattering between partons from nucleus-nucleus collisions at relativistic energies. To do this we must note that the experimental data are given for a particular centrality. To take this into account we introduce the centrality parameter, which depends on the maximum impact parameter b_m. The photon yield from hard collisions is then calculated from the expression

$$
\frac{dN_{\text{AB}}}{d^2 p_T\, dy}(b_m) = \mathcal{R}(b_m)\left[\frac{d\sigma_{\gamma,\text{hard}}}{d^2 p_T\, dy} + \frac{d\sigma_{\gamma,\text{frag}}}{d^2 p_T\, dy}\right], \tag{5}
$$

where $\mathcal{R}(b_m) \equiv \langle AB T_{\text{AB}} \rangle = \frac{\int_0^{b_m} d^2\mathbf{b}\, AB\, T_{\text{AB}}(b)}{\int_0^{b_m} d\mathbf{b}\,(\,1 - [1 - T_{\text{AB}}(b)\sigma_{NN}^{\text{in}}]^{AB})}$ and $T_{\text{AB}}(\mathbf{b}) = \int d^2\mathbf{s}\, T_{\text{A}}(\mathbf{s})\, T_{\text{B}}(\mathbf{b} - \mathbf{s})$ is the nuclear overlap function. For 0–10 % centrality we obtain $\mathcal{R} \sim 21.7\ \text{mb}^{-1}$. Before going to the numerical evaluation of the static photon rate, we plot the running coupling in Fig. 1, where the parametrization for $\alpha_s(k, T)$ is taken from Ref. [7]. It is seen that the value of the coupling is largest when $k \sim T$. For $k \gg T$ it agrees well with the temperature-dependent coupling. These features of α_s have important consequences on the photon production rate, as we see below.

The static photon rate is obtained from Eq. (3) using the running coupling. For $T = 200$ MeV the rates are shown in Fig. 2. The photon emission rate is enhanced by a factor of 1.7–6 compared to the case when the momentum dependence of the strong coupling is neglected.

Photons are produced at all stages of the collision and so it is necessary to integrate the emission rates over the space-time volume from creation to freeze-out. We assume that quark

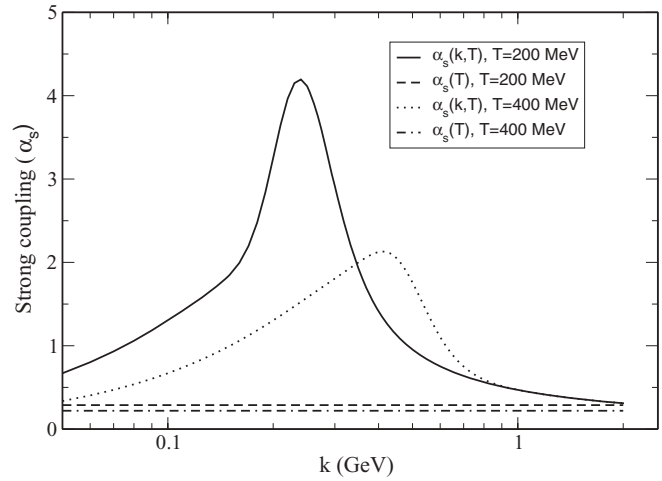

FIG. 1. Strong coupling as a function of momentum scale at two different temperatures [7].

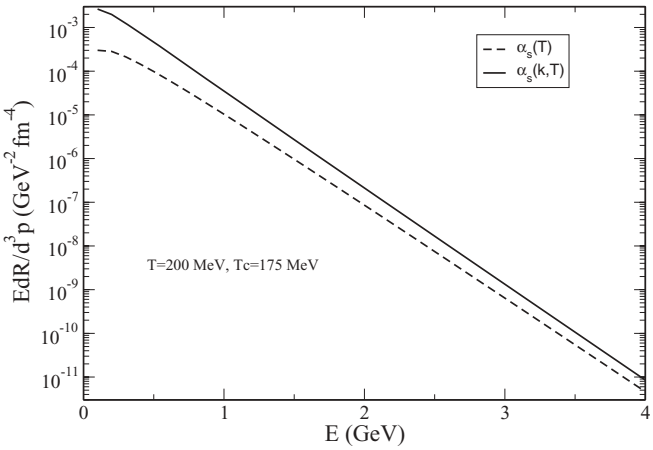

FIG. 2. Static photon rate with and without the running coupling.

gluon plasma having a temperature T_i is produced at an initial time τ_i. Hydrodynamic expansion and cooling follows up to a temperature T_c, where QGP crosses over to a hadronic gas. Subsequent cooling leads to freeze-out of the fluid element into observable hadrons. In the present work the fireball is taken to undergo an azimuthally symmetric transverse expansion along with a boost-invariant longitudinal expansion. The local temperature of the fluid element and the associated flow velocity as a function of the radial coordinate and proper time is obtained by solving the energy momentum conservation equation $\partial_\mu T^{\mu\nu} = 0$, where $T^{\mu\nu} = (\epsilon + P)u^\mu u^\nu + g^{\mu\nu}P$ is the energy momentum tensor for an ideal fluid. This set of equations is closed with the equation of state (EOS), typically a functional relation between the pressure P and the energy density ϵ. It is a crucial input which essentially controls the profile of expansion of the fireball. To minimize model dependencies we take the EOS from the lattice calculations of the Wuppertal-Budapest Collaboration [17].

The initial temperature is related to the experimentally measured hadron multiplicity through entropy conservation [18] as $T_i^3(b_m)\tau_i = \frac{2\pi^4}{45\zeta(3)\pi\ R_A^2 4a_k}\langle\frac{dN}{dy}(b_m)\rangle$, where $\langle dN/dy(b_m)\rangle$ is the hadron (predominantly pions) multiplicity for a given centrality class with maximum impact parameter b_m, R_A is the transverse dimension of the system, and a_k is the degeneracy of the system created. The hadron multiplicity resulting from Au + Au collisions is related to that from pp collisions at a given impact parameter and collision energy through the relation $\langle\frac{dN}{dy}(b_m)\rangle = [(1-x)\langle N_{\rm part}(b_m)\rangle/2 + x\langle N_{\rm coll}(b_m)\rangle]\frac{dN_{pp}}{dy}$, where x is the fraction of hard collisions. $\langle N_{\rm part}\rangle$ is the average number of participants and $\langle N_{\rm coll}\rangle$ is the average number of collisions evaluated by using the Glauber model; $dN_{pp}^{\rm ch}/dy = 2.5 - 0.25\ln s + 0.023\ln^2 s$ is the multiplicity of the produced hadrons in pp collisions at center-of-mass energy $\sqrt{s}$ [19]. We have assumed that 20% hard (i.e., $x = 0.20$) and 80% soft collisions are responsible for initial entropy production. Considering 0–10% centrality we get $T_i = 400$ MeV for $\tau_i = 0.2$ fm/c. One also requires the initial energy density and radial velocity profiles, which are taken respectively as [20] $\epsilon(\tau_i, r) = \frac{\epsilon_0}{1+e^{(r-R_A)/\delta}}$ and $v(\tau_i, r) = v_0[1 - \frac{1}{1+e^{(r-R_A)/\delta}}]$, where δ (∼0.5 fm) is a parameter known as the surface thickness. As

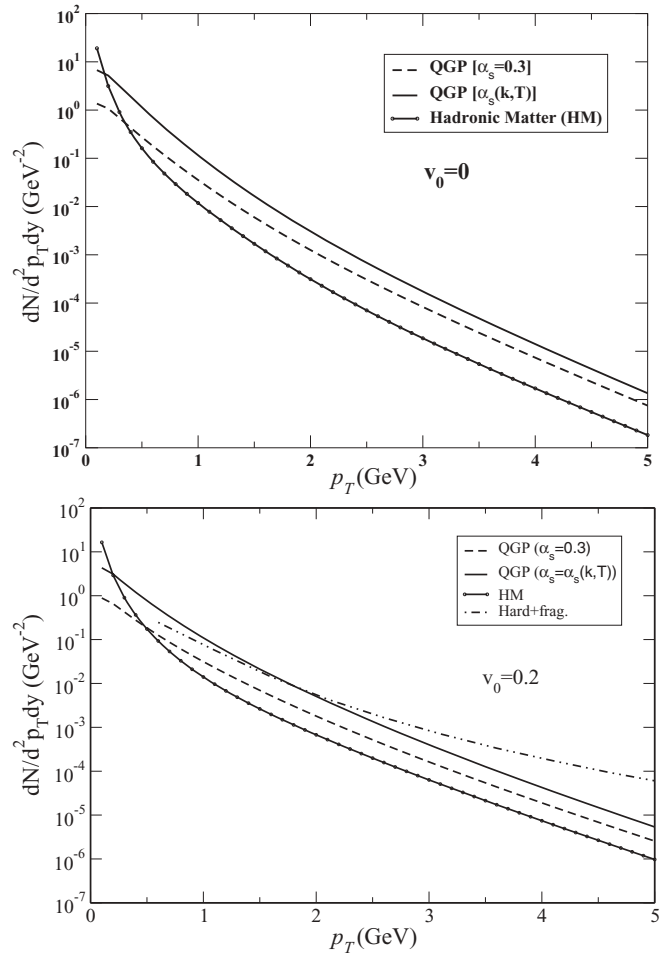

FIG. 3. Thermal photon p_T distributions for $T_i = 400$ MeV and $\tau_i = 0.2$ fm/c at central rapidity. The upper panel corresponds to $v_0 = 0$. Individual contribution from hard and fragmentation photons is shown in the lower panel for $v_0 = 0.2$.

discussed in Ref. [20], this choice of the initial fluid velocity profile is motivated by the fact that for a physical system the initial fluid velocity is zero inside the matter which approaches a value v_0 which is of the order of a typical particle transverse velocity in the diffuse region outside the matter distribution.

The other inputs are the transition temperature T_c, which is taken as 175 MeV as obtained from lattice QCD [21,22], and the freeze-out temperature T_f, which is taken to be 120 MeV. We now plot the thermal photon yield from both QGP and hot hadronic matter in Fig. 3 for $v_0 = 0$ and 0.2 in the left- and right-hand panels. At very low $p_T \sim 0.5$ GeV, the contribution from hadronic matter dominates. Beyond that the QGP contribution starts to take over. Interestingly, the effect of running coupling on the thermal photon production from QGP does survive the space-time evolution and continues to be discernible in this p_T domain. The effect of nonzero initial velocity (v_0) is also visible in the upward shift of the spectra at higher p_T in the right-hand panel compared to the left-hand panel. Moreover, the relative separation between the QGP contributions with and without the running coupling appears to be independent of the space-time evolution scenarios

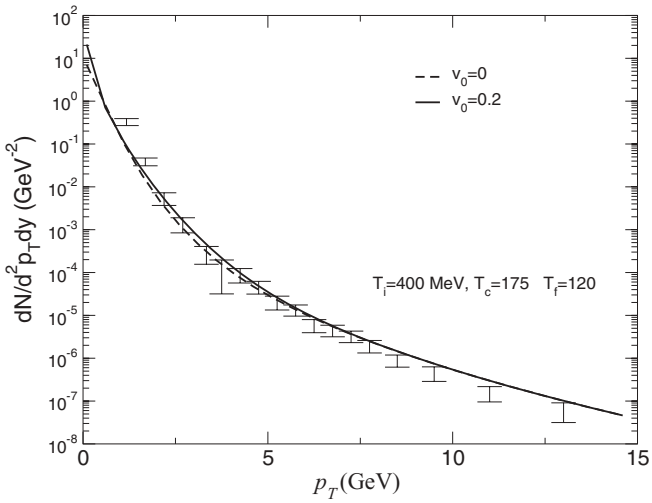

FIG. 4. Photon p_T distributions for $T_i = 400$ MeV and $\tau_i = 0.2$ fm/c at central rapidity. The data (for $|y| \leqslant 0.35$) are taken from Ref. [23].

corresponding to $v_0 = 0$ and 0.2. To assess their relative importance in comparison to the thermal yield, we also show in the right-hand panel the contribution from hard QCD photons and photons produced from jet fragmentation. As shown by the dash-dotted line this contribution clearly dominates the photon yield beyond about 2 GeV. Below that the hard and fragmentation contributions are almost similar to the QGP contribution.

We now compare the total yield with the direct photon data from Au + Au collisions at the Relativistic Heavy Ion Collider (RHIC) obtained by the PHENIX Collaboration [23] in Fig. 4. It is observed that the data are best reproduced by assuming a small initial velocity of the order of 0.2 (solid line) compared to $v_0 = 0$ (dashed line). However, the curves for $\alpha_s = \alpha_s(T)$ and $\alpha_s = \alpha_s(k, T)$ have merged with each other, implying that the observed difference seen in the thermal photon contribution for the two cases has been washed away once the hard and fragmentation contributions are added. Such a result can be understood once we realize that the contribution at a given value of the transverse momentum, especially up to 2–3 GeV/c, is a superposition of contributions from QGP at temperatures from T_i to T_c, hadronic matter from T_c to T_f, as well as from hard scatterings. Although the QGP contribution clearly dominates for $p_T > 0.5$ GeV, observation of momentum dependence of the strong coupling in the transverse momentum spectra of single photons does not appear to be feasible as it is overshadowed by the contributions coming from initial hard collisions.

To summarize, we calculated the static photon rate from QGP due to Compton and annihilation processes using the temperature- and momentum-dependent strong coupling. The rate was then contrasted with the case where α_s depends only on the temperature of the system. It is found that the static photon rate enhances significantly if the running coupling is used. We then performed a space-time evolution using relativistic hydrodynamics with initial conditions for Au + Au collisions at 200 GeV/n at RHIC. The significant difference in the yields does survive the space-time evolution and can be observed in the *thermal* photon spectra. However, due to the large contributions coming from the initial hard collisions and jet fragmentation the single-photon data from PHENIX cannot distinguish between the scenarios with and without momentum dependence of the running coupling.

[1] J. Alam, S. Sarkar, P. Roy, T. Hatsuda, and B. Sinha, Ann. Phys. **286**, 159 (2000).
[2] J. Kapusta, P. Lichard, and D. Seibert, Phys. Rev. D **44**, 2774 (1991).
[3] R. D. Pisarski and E. Braaten, Nucl. Phys. B **337**, 569 (1990); **339**, 310 (1990).
[4] P. Aurenche, F. Gelis, H. Zaraket, and R. Kobes, Phys. Rev. D **58**, 085003 (1998).
[5] P. Aurenche, F. Gelis, and H. Zaraket, Phys. Rev. D **61**, 116001 (2000); **62**, 096012 (2000).
[6] P. Arnold, G. D. Moore, and L. G. Yaffe, J. High Energy Phys. 11(2001) 057; 12 (2001) 009; 06 (2002) 030; T. Renk, Phys. Rev. C **67**, 064901 (2003).
[7] J. Braun and H.-J. Pirner, Phys. Rev. D **75**, 054031 (2007).
[8] P. B. Gossiaux and J. Aichelin, Phys. Rev. C **78**, 014904 (2008).
[9] K. Kajantie and P. V. Ruuskanen, Phys. Lett. B **121**, 352 (1983).
[10] C. Y. Wong and H. Wang, Phys. Rev. C **58**, 376 (1998).
[11] S. Sarkar, J. Alam, P. Roy, A. K. Dutt-Mazumder, B. Dutta-Roy, and B. Sinha, Nucl. Phys. A **634**, 206 (1998).
[12] P. Roy, S. Sarkar, J. Alam, and B. Sinha, Nucl. Phys. A **653**, 277 (1999).
[13] S. Turbide, R. Rapp, and C. Gale, Phys. Rev. C **69**, 014903 (2004).
[14] J. Pumplin, D. R. Stump, J. Huston, H. L. Lai, P. Nadolsky, and W. K. Tung, J. High Energy Phys. 012 (2002) 0207.
[15] J. F. Owens, Rev. Mod. Phys. **59**, 465 (1987).
[16] K. J. Eskola and K. Tuominen, Phys. Rev. D **63**, 114006 (2001).
[17] S. Borsányi, G. Endrődi, Z. Fodor, A. Jakovác, S. D. Katz, S. Krieg, C. Ratti, and K. K. Szabó, J. High Energy Phys. 10 (2010) 077.
[18] R. C. Hwa and K. Kajantie, Phys. Rev. D **32**, 1109 (1985).
[19] D. Khazreev and M. Nardi, Phys. Lett. B **507**, 121 (2001).
[20] H. von Gersdorff, L. McLerran, M. Kataja, and P. V. Ruuskanen, Phys. Rev. D **34**, 794 (1986).
[21] S. Katz, Nucl. Phys. A **774**, 159 (2006).
[22] M. Cheng, N. H. Christ, S. Datta, J. van der Heide, C. Jung, F. Karsch, O. Kaczmarek, E. Laermann, R. D. Mawhinney, C. Miao, P. Petreczky, K. Petrov, C. Schmidt, and T. Umeda, Phys. Rev. D **74**, 054507 (2006).
[23] S. S. Adler *et al.*, Phys. Rev. Lett. **94**, 232301 (2005); **98**, 012002 (2007); A. Adare *et al.* (PHENIX Collaboration), *ibid.* **104**, 132301 (2010).